

Supporting Information for

**Inorganic Lead-Free B- $\gamma$ -CsSnI<sub>3</sub> Perovskite Solar Cells Using Diverse**

**Electron-Transporting Materials: A Simulation Study**

Shuo Lin<sup>a</sup>, Baoping Zhang<sup>b</sup>, Tie-Yu Lü<sup>c</sup>, Jin-Cheng Zheng<sup>c,d,\*</sup>, Huaqing Pan<sup>e</sup>, Huanting Chen<sup>a</sup>, Chuanjin Lin<sup>a</sup>, Xirong Li<sup>a</sup>, Jinrong Zhou<sup>a</sup>

<sup>a</sup>College of Physics and Information Engineering, Minnan Normal University, Zhangzhou 363000, Fujian, People's Republic of China

<sup>b</sup>Department of Electronic Engineering, Optoelectronics Engineering Research Center, College of Electronic Science and Technology

(National Model Microelectronics College), Xiamen University, Xiamen, 361005, China

<sup>c</sup>Collaborative Innovation Center for Optoelectronic Semiconductors and Efficient Devices, Department of Physics, Xiamen University, Xiamen 361005, China

<sup>d</sup>Department of Physics, Xiamen University Malaysia, Sepang 43900, Selangor, Malaysia

<sup>e</sup>Department of Mechanical Engineering, Shangrao Vocational and Technical College, Shangrao 334109, Jiangxi, People's Republic of China

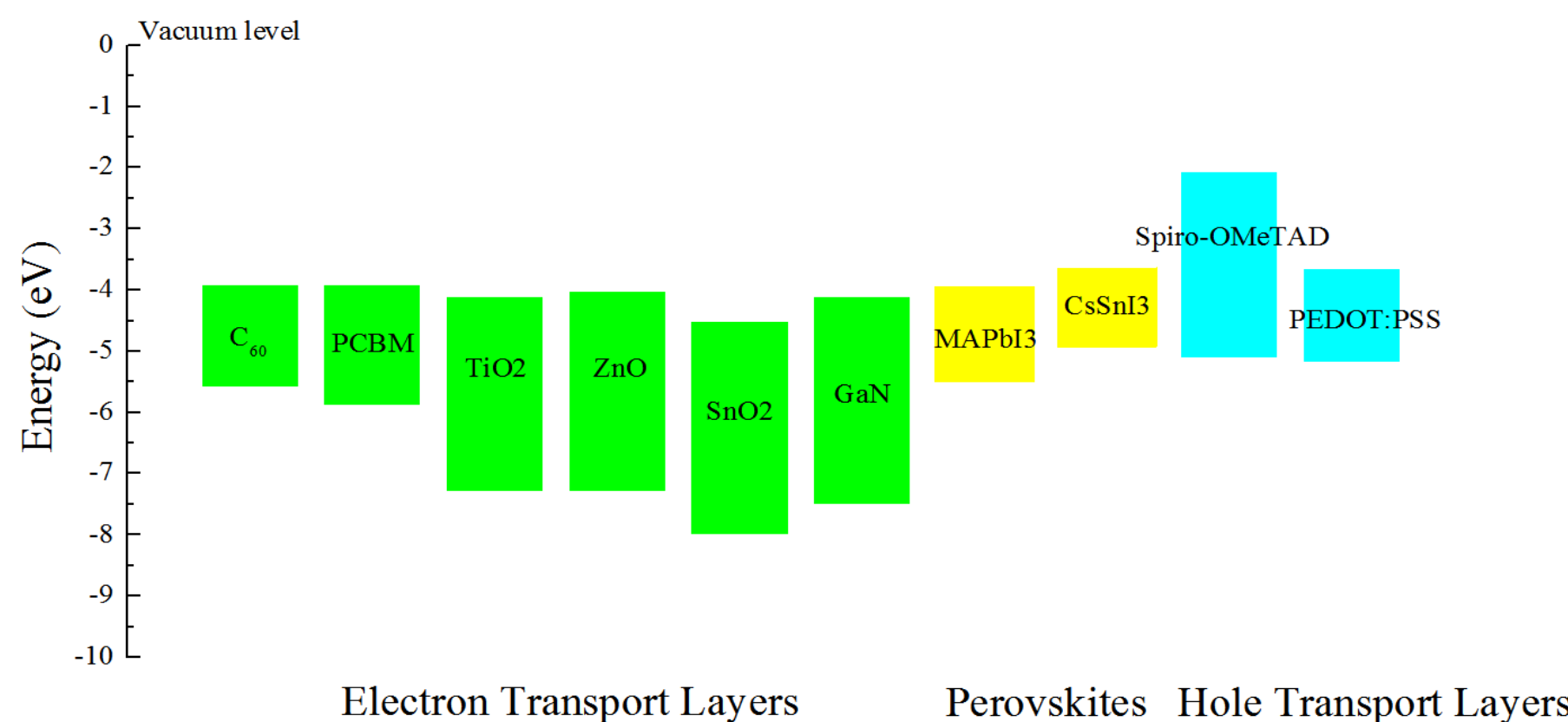
\*Corresponding author

E-mail address: jczheng@xmu.edu.cn (Jin-Cheng Zheng)

Table S1. Material parameters used in the simulation

Parameters	CsSnI <sub>3</sub>	TiO <sub>2</sub>	ZnO	SnO <sub>2</sub>	GaN	C <sub>60</sub>	PCBM	Spiro-OMeTAD	PEDOT:PSS
Band gap E <sub>g</sub> (eV)	1.3 [1]	3.2 [1]	3.3 [13]	3.5 [18]	3.4 [21]	1.7 [28]	2 [33]	3.06 [36]	1.55 [34]
Electron affinity $\chi$ (eV)	3.62 [1]	4.1 [7]	4 [13]	4.5 [18]	4.1 [22]	3.9 [29]	3.9 [33]	2.05 [36]	3.63 [34]
Dielectric constant $\epsilon$	48.2 [2]	55 [8]	8.656 [14]	9 [18]	9.5 [23]	4.25 [28]	4 [33]	3 [37]	3 [40]
Electron/hole mobility (cm <sup>2</sup> /V/s)	50/400 [3, 4]	0.006/0.006 [9]	100/25 [14]	100/25 [18]	Caughey-Thomas approximation (doping concentration dependent) [24]	1.6/1.6 [28]	0.01/0.01 [33]	2.00E-04/2.00E-4 [37]	9.00E-03/9.00E-3 [40]
Effective density of states in the conduction band N <sub>C</sub> (cm <sup>-3</sup> )	1.57E+19 [5]	1.00E+21 [9]	2.20E+18 [15]	2.20E+18 [18]	2.30E+18 [23]	1.44E+21 [30]	1.00E+21 [33]	1.00E+19 [38]	1.00E+19 [40]
Effective density of states in the valence band N <sub>V</sub> (cm <sup>-3</sup> )	1.47E+18 [5]	2.00E+20 [9]	1.80E+19 [15]	1.80E+19 [18]	4.60E+19 [23]	1.44E+21 [30]	2.00E+20 [33]	1.00E+19 [38]	1.00E+19 [40]
Minority lifetime	6.6 ns [3]	15 ms [10]	1 ns [16]	2.27 ns [19]	0.1 ns (for electrons) [25], 6.5 ns (for holes) [26]	1 $\mu$ s [31]	1 $\mu$ s [34]	0.1 $\mu$ s [38]	1 $\mu$ s [34]
Surface recombination velocities (cm/s)	2000 [3]	12 [11]	13 [11]	265 [11]	50000 [27]	4600 (assumed to be the same as PCBM)	4600 [11]	3100 [11]	4900 [11]
Absorption coefficient (1/cm <sup>-1</sup> )	[6]	[12]	[17]	[20]	[21]	[32]	[35]	[39]	[41]
Initial donor concentration (cm <sup>-3</sup> )	0	5E+19	1E+18	1E+18	1E+18	5E+17	5E+17	0	0
Optimal donor concentration (cm <sup>-3</sup> )	0	1E+21	1E+18	1E+18	1E+18	5E+18	5E+18	0	0
Initial acceptor concentration (cm <sup>-3</sup> )	5E+17 [3]	0	0	0	0	0	0	3E+17	1E+20
Initial thickness (nm)	variable	25	25	25	25	30	30	400	40
Optimal thickness (nm)	100~200								

Figure S1. Energy band alignment of all contact materials and CsSnI<sub>3</sub> adopted in this study



## References

- [1] Chung, I.; Lee, B.; He, J.; Chang, R. P. H.; Kanatzidis, M. G. All-solid-state dye-sensitized solar cells with high efficiency. *Nature* **2012**, *485*, 486-489.
- [2] Kumar, M. H.; Dharani, S.; Leong, W. L.; Boix, P. P.; Prabhakar, R. R.; Baikie, T.; Shi, C.; Ding, H.; Ramesh, R.; Asta, M.; Graetzel M.; Mhaisalkar, S. G.; Mathews, N. Lead-free halide perovskite solar cells with high photocurrents realized through vacancy modulation. *Adv. Mater.* **2014**, *26*, 7122-7127.
- [3] Wu, B.; Zhou, Y.; Xing, G.; Xu, Q.; Garces, H. F.; Solanki, A.; Goh, T. W.; Padture, N. P.; Sum, T. C. Long minority-carrier diffusion length and low surface-recombination velocity in inorganic lead-free CsSnI<sub>3</sub> perovskite crystal for solar cells. *Adv. Funct. Mater.* **2017**, *27*, 1604818.
- [4] Chung, I.; Song, J. H.; Im, J.; Androulakis, J.; Malliakas, C. D.; Li, H.; Freeman, A. J.; Kenney, J. T.; Kanatzidis, M. G. CsSnI<sub>3</sub>: semiconductor or metal? High electrical conductivity and strong near-infrared photoluminescence from a single material. High hole mobility and phase-transitions. *J. Am. Chem. Soc.* **2012**, *134*, 8579-8587.
- [5] Shum, K.; Chen, Z.; Qureshi, J.; Yu, C.; Wang, J. J.; Pfenninger, W.; Vockic, N.; Midgley, J.; Kenney, J. T. Synthesis and characterization of CsSnI<sub>3</sub> thin films. *Appl. Phys. Lett.* **2010**, *96*, 221903.
- [6] Qiu, X.; Cao, B.; Yuan, S.; Chen, X.; Qiu, Z.; Jiang, Y.; Ye, Q.; Wang, H.; Zeng, H.; Liu, J.; Kanatzidis, M. G. From unstable CsSnI<sub>3</sub> to air-stable Cs<sub>2</sub>SnI<sub>6</sub>: A lead-free perovskite solar cell light absorber with bandgap of 1.48 eV and high absorption coefficient. *Sol. Energy Mater. Sol. Cells* **2017**, *159*, 227-234.
- [7] Jung, H. S.; Park, N. G. Perovskite solar cells: from materials to devices. *Small* **2015**, *11*, 10-25.
- [8] van de Krol, R.; Goossens, A.; Schoonman, J. Mott-Schottky analysis of nanometer-scale thin-film anatase TiO<sub>2</sub>. *J. Electrochem. Soc.* **1997**, *144*, 1723-1727.
- [9] Adhikari, K. R.; Gurung, S.; Bhattacharai, B. K.; Soucase, B. M. Comparative study on MAPbI<sub>3</sub> based solar cells using different electron transporting materials. *Phys. Status Solidi C* **2016**, *13*, 13-17.
- [10] Mitroi, M. R.; Fara, L. Optimization of black dye-sensitized solar cells by numerical simulation. *J. Renewable Sustainable Energy* **2013**, *5*, 041818.
- [11] Wang, J.; Fu, W.; Jariwala, S.; Sinha, I.; Jen, AK-Y.; Ginger, D. S. Reducing surface recombination velocities at the electrical contacts will improve perovskite photovoltaics. *ACS Energy Lett.* **2019**, *4*, 222-227.
- [12] Naik, V. M.; Haddad, D.; Naik, R.; Benci, J.; Auner, G. W. Optical properties of anatase, rutile and amorphous phases of TiO<sub>2</sub> thin films grown at room temperature by RF magnetron sputtering. *Mat. Res. Soc. Symp. Proc.* **2003**, *755*, DD11.12.1. Materials Research Society.
- [13] Bansal, S.; Aryal, P. Evaluation of new materials for electron and hole transport layers in perovskite-based solar cells through SCAPS-1D simulations. *IEEE 44th photovoltaic specialists conference* **2017**. IEEE.
- [14] Pearton, S. J.; Norton, D. P.; Ip, K.; Heo, Y. W.; Steiner, T. Recent progress in processing and properties of ZnO. *Superlattice Microst.* **2003**, *34*, 3-32.
- [15] Wanda, M. D.; Ouédraogo, S.; Tchoffo, F.; Zougmoré, F.; Ndjaka, J. M. B. Numerical investigations and analysis of Cu<sub>2</sub>ZnSnS<sub>4</sub> based solar cells by SCAPS-1D. *Int. J. photoenergy* **2016**, 2152018.
- [16] Ali, A.; Hussain, B.; Ebong, A. Computer modeling of n-ZnO/p-Si single heterojunction bifacial solar cell. *IEEE 43rd Photovoltaic Specialists Conference* **2016**. IEEE.
- [17] SCAPS-1D software data file.
- [18] Cao, Y.; Zhu, X. Y.; Chen, H. B.; Wang, C. G.; Zhang, X. T.; Hou, B. D.; et al. Simulation and optimal design of antimony selenide thin film solar cells. *Acta. Phys. Sin.* **2018**, *67*, 247301.
- [19] Lee, P. M.; Liao, C. H.; Lin, C. H.; Liu, C. Y. Photocurrent generation in SnO<sub>2</sub> thin film by surface charged chemisorption O ions. *Appl. Surf. Sci.* **2018**, *442*, 398-402.
- [20] Khan, A. F.; Mehmood, M.; Aslam, M.; Ashraf, M. Characteristics of electron beam evaporated nanocrystalline SnO<sub>2</sub> thin films annealed in air. *Appl. Surf. Sci.* **2010**, *256*, 2252-2258.
- [21] Muth, J. F.; Lee, J. H.; Shmagin, I. K.; Kolbas, R. M.; Casey, H. C.; Jr.; Keller, B. P.; Mishra, U. K.; DenBaars, S. P. Absorption coefficient, energy gap, exciton binding energy, and recombination lifetime of GaN obtained from transmission measurements. *Appl. Phys. Lett.* **1997**, *71*, 2572-2524.

- [22] Martí, A.; Tablero, C.; Antolin, E.; Luque, A.; Campion, R. P.; Novikov, S. V.; Campion, R. P.; Novikov, S. V.; Foxon, C. T. Sol. Energy Mater. Sol. Cells **2009**, *93*, 641-644.
- [23] Lin, S.; Zeng S. W.; Cai X. M.; Zhang J. Y.; Wu S. X.; Sun L.; Zhang, B. P. Simulation of doping levels and deep levels in InGaN-based single-junction solar cell. J. Mater. Sci. **2012**, *47*, 4595-4603.
- [24] Mnatsakanov, T. T.; Levenshtein, M. E.; Pomortseva, L. I.; Yurkov, S. N.; Simin, G. S., Khan, M. A. Carrier mobility model for GaN. Solid-State Electron. **2003**, *47*, 111–115.
- [25] Bandic, Z. Z.; Bridger, P. M.; Piquette, E. C.; McGill, T. C. Electron diffusion length and lifetime in p-type GaN. Appl. Phys. Lett. **1998**, *73*, 3276-3278.
- [26] Bandic, Z. Z.; Bridger, P. M.; Piquette, E. C.; McGill, T. C. Minority carrier diffusion length and lifetime in GaN. Appl. Phys. Lett. **1998**, *72*, 3166-3168.
- [27] Aleksiejunas, R.; Sudzius, M.; Malinauskas, T.; Vaitkus, J.; Jarasiunas, K.; Sakai, S. Appl. Phys. Lett. **2003**, *83*, 1157-1159.
- [28] Golubev, T.; Liu, D.; Lunt, R.; Duxbury, P. Understanding the impact of C<sub>60</sub> at the interface of perovskite solar cells via drift-diffusion modeling. AIP Adv. **2019**, *9*, 035026.
- [29] Liang, P. W.; Chueh, C. C.; Williams, S. T.; Jen, A. K. -Y. Roles of fullerene-based interlayers in enhancing the performance of organometal perovskite thin-film solar cells. Adv. Energy Mater. **2015**, *5*, 1402321.
- [30] Dixit, H.; Punetha, D.; Pandey, S. K. Improvement in performance of lead free inverted perovskite solar cell by optimization of solar parameters. Optik **2019**, *179*, 969-976.
- [31] Burlingame, Q.; Tong, X.; Hankett, J.; Slootsky, M.; Chen, Z.; Forrest, S. R. Photochemical origins of burn-in degradation in small molecular weight organic photovoltaic cells. Energy Environ. Sci. **2015**, *8*, 1005-1010.
- [32] Monestier, F.; Simon, J. J.; Torchio, P.; Escoubas, L.; Ratier, B.; Hojeij, W.; Lucas, B.; Moliton, A.; Cathelinaud, M.; Defranoux, C.; Flory, F. Optical modeling of organic solar cells based on CuPc and C60. Appl. Optics **2008**, *47*, C251-6.
- [33] Zhao, P.; Liu, Z.; Lin, Z.; Chen, D.; Su, J.; Zhang, C.; Zhang, J.; Chang, J.; Hao, Y. Device simulation of inverted CH<sub>3</sub>NH<sub>3</sub>PbI<sub>3-x</sub>Cl<sub>x</sub> perovskite solar cells based on PCBM electron transport layer and NiO hole transport layer. Sol. Energy **2018**, *169*, 11-18.
- [34] Nie, W.; Tsai, H.; Asadpour, R.; Blancon, J. C.; Neukirch, A. J.; Gupta, G.; Crochet, J. J.; Chhowalla, M.; Tretiak, S.; Alam, M. A.; Wang, H.-L.; Mohite, A. D. High-efficiency solution-processed perovskite solar cells with millimeter-scale grains. Science **2015**, *347*, 522.
- [35] Pospisil, J.; Schmiedova, V.; Zmeskal, O.; Cerny, J. Study of optical and electrical properties of organic thin films for photovoltaic applications. Mater. Sci. **2015**, *21*, 333-338.
- [36] Hossain, M. I.; Alharbi, F. H.; Tabet, N. Copper oxide as inorganic hole transport material for lead halide perovskite based solar cells. Sol. Energy **2015**, *120*, 370-380.
- [37] Minemoto, T.; Murata, M. Device modeling of perovskite solar cells based on structural similarity with thin film inorganic semiconductor solar cells. J. Appl. Phys. **2014**, *116*, 054505.
- [38] An, Y.; Shang, A.; Cao, G.; Wu, S.; Ma, D.; Li, X. Perovskite Solar Cells: Optoelectronic Simulation and Optimization. Sol. RRL **2018**, *2*, 1800126.
- [39] Filipič, M.; Löper, P.; Niesen, B.; Wolf, S. D.; Krč, J.; Ballif, C.; Topič, M. Opt. Express **2015**, *23*, A263-78.
- [40] Olyaeefar, B.; Ahmadi-Kandjani, S.; Asgari, A. Classical modelling of grain size and boundary effects in polycrystalline perovskite solar cells. Sol. Energy Mater. Sol. Cells **2018**, *180*, 76-82.
- [41] [http://www.ampsmodeling.org/materials/PEDOT\\_absorption\\_coefficients.htm](http://www.ampsmodeling.org/materials/PEDOT_absorption_coefficients.htm). Accessed Sep 2010.